Additive manufactured compliant surface reflectance sensor

Teemu Salo, Maija Luukko, Aki Halme and Jukka Vanhala
Information Technology and Communication Sciences, Tampere University, Tampere, Finland
Email: teemu.salo@tuni.fi, jukka.vanhala@tuni.fi

***Abstract*—In this paper[1], we present an additive manufacturing (AM) method to implement structural electronics using an off-the-shelf fused deposition modeling (FDM) 3D printer with thermoplastic polyurethane (TPU) filament, conductive silver ink, and electronics components in standard packages. As a demonstrator, a surface reflectance sensor has been implemented. The structure consists of several 3D-printed TPU layers, 3D channels for the conductors, and cavities for components. A comparison is made between the performance of a traditional implementation on rigid PCB and the new sensor. The study shows that the chosen approach can be used for AM structural electronics.**

Keywords—additive manufacturing, structural electronics, 3D-printed electronics, compliant electronics.

I. INTRODUCTION

In the last two decades, additive manufacturing (AM) has revolutionized single and small-series production in the plastics and metal industries. The advantages, such as the high complexity of designs, easiness to add user-specified mass customization, and wide range of materials have established the role of AM in the production of tailored high-tech parts [1]. The parts can have high strength, stretchability, heat resistance, and other advanced properties [2]. However, despite the wide usage of AM, the AM revolution for functional parts has not happened yet. Especially in the hybrid field of 3D-printed electronics, there are three areas, which are still limiting the expansion of the field.

The first limitation is (1) the current way to design 3D-printed electronics. The traditional printed circuit boards (PCBs) have electronic components on the top side or top and bottom sides of the boards, which limit the component density and routing options. In addition, the mechanical deformability of the PCBs is typically uniformly rigid, flexible, or flexible with local rigid areas [3]. These current methods and design programs are not optimized for 3D-printed electronics, where the location and orientation of the electronic components are not restricted planarly [4]. The freedom to freely choose the orientation of the components potentially increases the density of the components and shortens the length of the routings between the components [5].

The second restriction is (2) current 3D-printing materials. AM of metals can require debinding and sintering processes, which cause difficulties for 3D-printed electronics fabrication. For example, with 316L steel, the manufacturing process temperatures increase up to 1360 °C [6]. On the contrary in the plastics AM, the low-temperature resistance of the most used plastics hinders the usage of conventional electronics processes [7]. The varying chemical resistance of the plastics also makes the photolithography processes of PCBs challenging [8]. There has been promising development of conductive materials for fused deposition modeling (FDM) by mixing conductive fillers inside plastic filaments [9], feeding thin conductive filament yarns along the molten plastic extrusion [10], and filling 3D-printed hollow tubes with liquid metal [11]. Despite functional demonstrations, the methods suffer from relatively low conductivity and high surface resistance, design restrictions, and electrical joining difficulties, correspondingly.

The third current limitation is (3) the commercial AM technology. The machines for 3D printed electronics use different 3D printing methods, which have their own materials and advantages and disadvantages. For example, in FDM, sensor and other electronic structures are realized with process-compatible conductive filaments [12,13], but more complex features are integrated with inserts or printed with inks by direct ink writing (DIW) and material jetting (MJ) [14-18]. DIW enables the use of silicones, inks, liquid metals, and other liquid-form materials, but truly free-form shapes are challenging [19,20]. Currently, the most promising commercial machine development has been realized by Nano Dimension [17] and Neotech AMT [18].

In this paper, we demonstrate a 3D-structural surface reflectance sensor (later sensor), which is built by AM methods. The demonstration is done by using a commercial tabletop FDM machine for the printing of the compliant plastic part of the sensor. The interconnections and off-the-shelf electronic components are added inside the structure by pausing the 3D-printing process at specific layers, which process can be done automatically with a more sophisticated Neotech AMT machine. The modified commercial FDM process enables cost-efficient, more straightforward, and mechanically complex structural electronics, which can be used in stretchable and wearable applications.

II. DESIGN CONSIDERATIONS

The fabrication of 3D-printable electronics is started by considering design limitations and possibilities. First, the combability of the plastic and the conductive ink is optimized by choosing a thermoplastic polyurethane (TPU)

[1]This paper was funded by the Academic of Finland under the project REEL, decision number 334175.

filament (white Ultimaker TPU 95A by Ultimaker BV) and a conductive silver ink with a TPU binder (CI-1036, by ECM). The same polymer matrix promotes adhesion and common thermal expansion between the materials. Also, TPU is deformable and has good thermal resistance, which makes it usable for stretchable and wearable electronics applications [21]. Especially for AM wearables, the 3D-printed TPU filament is compatible with textile substrates, either directly printed on textile [22], or directly printed on TPU film, which is further laminated on textile [23]. After the material optimization, the circuitry of the sensor is designed (Fig. 1).

In Fig 1., J1 is the power source connector, R1 and R2 are the resistors, D1 is 599 series LED (by Dialight), T1 is an SFH 3711 phototransistor (by OSRAM Opto Semiconductors GmbH), C1 is the capacitor, and V_{OUT} is the measurement point. The size of the components is 1206, except the size of the phototransistor is 0805. Supply voltage is 5V.

In the design, the placement of the ink inside the 3D-printed part has to be considered by preparing channels and vias inside the part. Since the electrical components are also placed in the channels, the height of the channels needs to be at least the height of the largest used component. The sufficient channel height also protects the ink in the channels. In FDM, the printed molten bead, especially from soft filaments like TPU, tends to fall into the channels during the 3D printing of the first layer of the channel's roof. The phenomenon can be limited by minimizing the width of the channels. Vias, on the contrary, should be optimized with the viscosity of the ink, whereas high viscose inks require larger vias. The ink flow into the vias can be improved by using sloped vias instead of traditionally vertically penetrating vias. Fig. 2 shows the 3D design of the sensor part.

III. PREPARATION OF THE SENSOR

A. Fabrication of the 3D-structural and PCB sensors

The fabrication of the sensor is started by preparing the 3D design with Solidworks 2021 (by Dassault Systemes), and generating a printing program with Ultimaker Cura 5.1.0 (by Ultimaker BV) for the FDM machine Ultimaker 3 (by Ultimaker BV). For the 3D-printing, 0.15 mm layer height, 0.4 mm nozzle diameter, 230 °C nozzle temperature, 60 °C glass plate temperature, 20 mm/min general printing speed, 100 % infill density, lines infill pattern, and wall line count 2 are used. In addition to the conventional settings, two post-processing scripts are added to pause the printing process

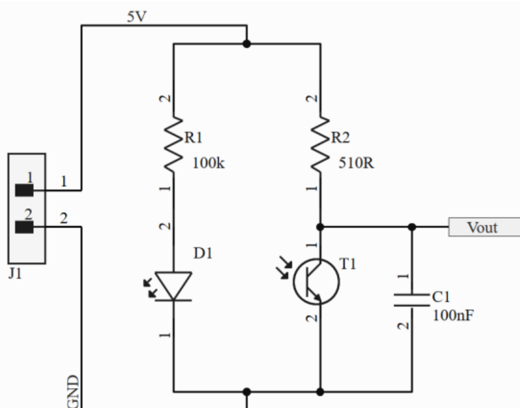

Fig. 1. The circuitry of the sensor.

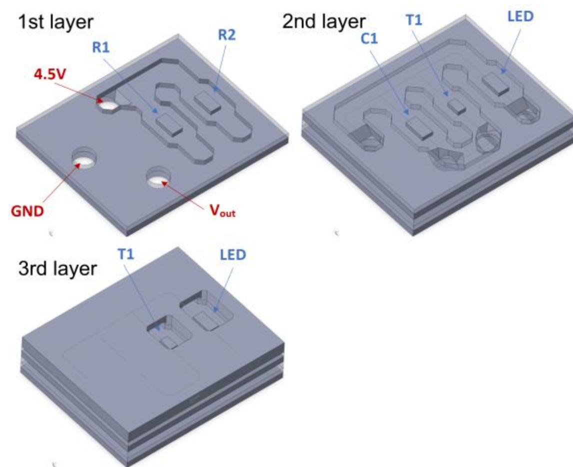

Fig. 2. The 3D design of the sensor. The structure is divided into three layers, where the process is paused between the parts to enable the addition of the conductive ink and components.

between 1st and 2nd layers, and 2nd and 3rd layers (Fig. 2). The inaccuracies because the leakage of TPU during the pause are prevented by using a sacrificial tower next to the sensor. The final size of the sensor is 25.7 mm * 21.2 mm * 6.6 mm. In the channels, the ink is dispensed manually with a syringe and the components are placed with tweezers. The ready 3D-printed part is heat treated in an oven at 125 °C for 30 min. Lastly, wires are soldered into three bottom contacts of the 1st layer. The width and height of the channels are 3.0 mm and 1.6 mm, correspondingly. Fig. 3a shows the unfinished 3D-structural sensor, and Fig. 3b shows the working sensor.

For the evaluation of the 3D-structural sensor, another sensor with similar components is prepared by using traditional PCB manufacturing methods (Fig. 3c). The design of the PCB is prepared with Altium 20.0.12 (by Altium LLC). The PCB manufacturing process includes a multi-step photolithography process, drilling, and soldering of wires. The main difference between the sensors is the location of the phototransistor; the phototransistor is on the surface of the PCB while the phototransistor in the 3D-structural sensor has a 2.0 mm indentation from the surface of the 3D-printed part. The effect of the indentation is further studied by fabricating an additional 3D-printed cover over the PCB sensor, which leaves a 1.5 mm indentation between the phototransistor and the surface of the 3D-printed cover (Fig. 3d). The cover is fixed on the PCB sensor.

B. The test method

The sensors can be used with different surface materials, which affects the voltage output of the sensors. The output voltage is the highest against the black surface and the lowest against the white surface. The reported spectral range of sensitivity of the phototransistors is 470 – 670 nm and the peak sensitivity is 570 nm corresponding to yellow color. The LED has a matching peak wavelength at 569 nm. For the testing of the prepared sensors, system-level testing is done by comparing the voltage output of the sensors with Tektronix TPS 2014 oscilloscope (by Tektronix). Table 1 shows the comparison colors of the sensors. For the testing, the color areas are printed on Antalis Image Volume 80 g white paper, which is adhered on a light-blocking cardboard supporting layer.

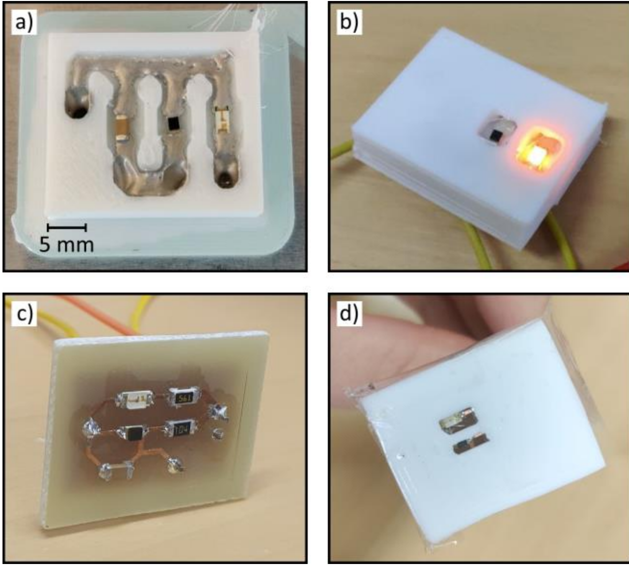

Fig. 3. Different tested sensors: a) unfinished 3D-structural sensor, b) finished 3D-structural sensor, c) PCB sensor, and d) covered PCB sensor.

TABLE I. COLORS USED IN THE COMPARISON OF THE SENSORS

Color	Color	CMYK color code			
		C	*M*	*Y*	*K*
Black		60	40	0	100
Red		0	100	100	0
Magenta		0	100	0	0
Blue		90	80	0	0
Turquoise		70	0	40	0
Green		70	0	100	0
Yellow		0	0	90	0
White		0	0	0	0

IV. RESULTS AND DISCUSSION

Fig. 4. shows that the output from the 3D-printed structural sensor corresponds very well with the output from the PCB sensor. The only difference is with the white surface. The results present that the same level readings are possible to achieve with traditional PCB manufacturing and AM methods, from which the AM has promising future applications because of the smaller material consumption, customizability, and wearability.

The results show that the response of the fabricated sensors varies despite the same electronic components, where the interconnections likely cause the difference in the conductivity. The voltage output of the PCB sensor is generally 0.1 V lower than the voltage output of the 3D-structural sensor. In the red and magenta spectrum, the difference is higher between 0.3 – 0.4 V. The highest difference is in the white color area, where the PCB sensor voltage output is 1.7 V smaller. The additional 3D-printed cover on the PCB sensor decreases the response of the PCB sensor by approximately 20 – 30 %, where the yellow and white color results are exceptions. The cover decreases the voltage output of the PCB sensor by ~ 50 %, while the difference in the white color area is minimal.

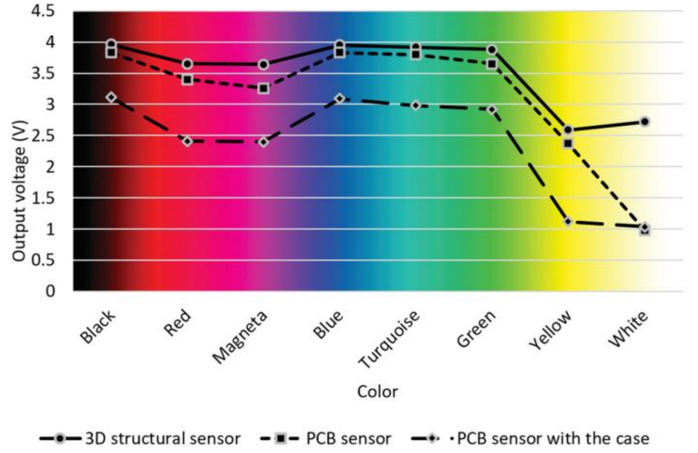

Fig. 4. Voltage output comparison of the sensors exposed with differently colored surfaces.

From Fig 3. and Fig. 4, it can be seen that there are two simultaneous phenomena that affect the output voltage of the sensors. First, by burying the LED in the 3D-structural and covered sensors (2.0 mm and 1.5 mm, correspondingly), the light exposure conditions of the phototransistor change. The high 2.0 mm indentation decreases the amount of light in the sensor, and the voltage output range is < 50 % of the total possible range (0 – 5 V). Only the 0.5 mm less deep covered PCB sensor receives more light, which is seen as the similar white color results of the covered and the traditional PCB sensors. However, it is possible, that the taped cover leaks light to the sensor, which together with the smaller indentation, generally decreases the voltage output of the sensor.

Secondly, the color of the plastic affects the sensor readings. The white-colored TPU plastic conducts the yellow light of the LED into the 3D-printed part (Fig. 3b). The higher amount of yellow light is seen as the lower voltage output of the 3D-structural and covered PCB sensors, which differs from the bare PCB sensor. Based on the results, darker and less clear plastics-based 3D-structural sensors can have even more similar behavior to the PCB sensor. Also, for future applications, the 3D-structural sensor can have multiple different colored LEDs instead of one LED. From the mechanical aspects, the compliance of the sensor can be improved by using softer TPU grades, thinner designs, and the position optimization of the electronic components.

V. CONCLUSION

The fabrication of 3D-structural electronics is a multi-stage process, which includes the optimization of materials, design, and manufacturing processes. By using TPU-based plastics and stretchable conductive inks, additive manufactured 3D-structural wearable electronics with powerful off-the-shelf electronic components can be prepared. Compared to the traditional rigid PCB sensor, the compliant 3D-structural sensor has corresponding system-level electrical properties. The 3D-structural design differs from the PCB design, which causes minor effects on the performance and brings out new process parameters. For example, the white color of the 3D-printed plastic part conducts yellow-colored light from the LED, which is seen from the voltage output of the sensor.

REFERENCES

[1] M. Attaran, “The rise of 3-D printing: The advantages of additive manufacturing over traditional manufacturing,” *Business Horizons*, vol. 60, no. 5, pp. 677–688, 2017.

[2] A. Cano-Vicent *et al.*, “Fused deposition modelling: current status, methodology, applications and future prospects,” *Addit. Manuf.*, vol. 47, 102378, 2021.

[3] S. Anastasova, P. Kassanos, and G.-Z. Yang, “Multi-parametric rigid and flexible, low-cost, disposable sensing platforms for biomedical applications,” *Biosens. Bioelectron.,* vol. 102, pp. 668–675, 2018.

[4] A. Panesar, D. Brackett, I. Ashcroft, R. Wildman, and R. Hague, “Design framework for multifunctional additive manufacturing: placement and routing of three-dimensional printed circuit volumes,” *J. Mech. Des.*, vol. 137, no. 11, 111414, 2015.

[5] G. T. Carranza, U. Robles, C. L. Valle, J. J. Gutierrez, and R. C. Rumpf, “Design and hybrid additive manufacturing of 3-D/volumetric electrical circuits,” *IEEE Trans. Compon., Packag. Manufact. Technol.*, vol. 9, no. 6, pp. 1176–1183, 2019.

[6] H. Ramazani and A. Kami, “Metal FDM, a new extrusion-based additive manufacturing technology for manufacturing of metallic parts: a review,” *Prog. Addit. Manuf.*, vol. 7, no. 4, pp. 609–626, 2022.

[7] M. Manoj Prabhakar *et al.*, “A short review on 3D printing methods, process parameters and materials,” *Mater. Today: Proc.*, vol. 45, pp. 6108–6114, 2021.

[8] I. T. S. Heikkinen *et al.*, “Chemical compatibility of fused filament fabrication-based 3-D printed components with solutions commonly used in semiconductor wet processing,” *Addit. Manuf.*, vol. 23, pp. 99–107, 2018.

[9] C. J. Hohimer, G. Petrossian, A. Ameli, C. Mo, and P. Pötschke, “3D printed conductive thermoplastic polyurethane/carbon nanotube composites for capacitive and piezoresistive sensing in soft pneumatic actuators,” *Addit. Manuf.*, vol. 34, 101281, 2020.

[10] L. Yin, X. Tian, Z. Shang, X. Wang, and Z. Hou, “Characterizations of continuous carbon fiber-reinforced composites for electromagnetic interference shielding fabricated by 3D printing,” *Appl. Phys. A*, vol. 125, no. 4, p. 266, 2019.

[11] Y. He *et al.*, “Three-dimensional coprinting of liquid metals for directly fabricating stretchable electronics,” *3D Print. Addit. Manuf.*, vol. 5, no. 3, pp. 195–203, 2018.

[12] K. Kim *et al.*, “3D printing of multiaxial force sensors using carbon nanotube (CNT)/thermoplastic polyurethane (TPU) filaments,” *Sens. Actuators A: Phys.*, vol. 263, pp. 493–500, 2017.

[13] M. Ntagios, H. Nassar, and R. Dahiya, “Closed-loop direct ink extruder system with multi-part materials mixing,” *Addit. Manuf.*, vol. 64, pp. 103437, 2023.

[14] K. Li *et al.*, “3D printed stretchable capacitive sensors for highly sensitive tactile and electrochemical sensing,” *Nanotechnology*, vol. 29, no. 18, 185501, 2018.

[15] A. D. Valentine *et al.*, “Hybrid 3D printing of soft electronics,” *Adv. Mater.*, vol. 29, no. 40, 1703817, 2017.

[16] T. Salo, D. Di Vito, A. Halme, and J. Vanhala, “Electromechanical properties of 3D-printed stretchable carbon fiber composites,” *Micromachines*, vol. 13, no. 10, 1732, 2022.

[17] J. Zhu *et al.*, “Additively manufactured millimeter-wave dual-band single-polarization shared aperture Fresnel zone plate metalens antenna,” *IEEE Trans. Antennas Propagat.*, vol. 69, no. 10, pp. 6261–6272, 2021.

[18] K. Lomakin *et al.*, “Evaluation and characterization of 3-D printed pyramid horn antennas utilizing different deposition techniques for conductive material,” *IEEE Trans. Compon., Packag. Manufact. Technol.*, vol. 8, no. 11, pp. 1998–2006, 2018.

[19] C. Votzke, U. Daalkhaijav, Y. Mengüç, and M. L. Johnston, “3D-printed liquid metal interconnects for stretchable electronics,” *IEEE Sens. J.*, vol. 19, no. 10, pp. 3832–3840, 2019.

[20] M. R. Binelli *et al.*, “Digital manufacturing of personalized footwear with embedded sensors,” *Sci. Rep.*, vol. 13, 1962, 2023.

[21] J. Suikkola *et al.*, “Screen-printing fabrication and characterization of stretchable electronics,” *Sci. Rep.*, vol. 6, no. 1, 25784, 2016.

[22] M. Korger *et al.*, “Testing thermoplastic elastomers selected as flexible three-dimensional printing materials for functional garment and technical textile applications,” *J. Eng. Fibers Fabr.*, vol. 15, p. 1–10, 2020.

[23] T. Salo, A. Halme, J. Lahtinen, and J. Vanhala, “Enhanced stretchable electronics made by fused-filament fabrication,” *Flex. Print. Electron.*, vol. 5, no. 4, 045001, 2020.